

Improved limits on a hypothetical $X(16.7)$ boson and a dark photon decaying into e^+e^- pairs

D. Banerjee,^{4,5} J. Bernhard,⁴ V. E. Burtsev,² A. G. Chumakov,¹³ D. Cooke,⁶ P. Crivelli,¹⁵ E. Depero,¹⁵ A. V. Dermenev,⁷ S. V. Donskov,¹¹ R. R. Dusaev,¹³ T. Enik,² N. Charitonidis,⁴ A. Feshchenko,² V. N. Frolov,² A. Gardikiotis,¹⁰ S. G. Gerassimov,^{8,3} S. N. Gninenko,⁷ M. Hösgen,¹ M. Jeckel,⁴ V. A. Kachanov,¹¹ A. E. Karneyeu,⁷ G. Kekelidze,² B. Ketzer,¹ D. V. Kirpichnikov,⁷ M. M. Kirsanov,⁷ V. N. Kolosov,¹¹ I. V. Konorov,^{8,3} S. G. Kovalenko,¹² V. A. Kramarenko,^{2,9} L. V. Kravchuk,⁷ N. V. Krasnikov,^{2,7} S. V. Kuleshov,¹² V. E. Lyubovitskij,^{13,14} V. Lysan,² V. A. Matveev,² Yu. V. Mikhailov,¹¹ L. Molina Bueno,¹⁵ D. V. Peshekhonov,² V. A. Polyakov,¹¹ B. Radics,¹⁵ R. Rojas,¹⁴ A. Rubbia,¹⁵ V. D. Samoylenko,¹¹ D. Shchukin,⁸ V. O. Tikhomirov,⁸ I. Tlisova,⁷ D. A. Tlisov,⁷ A. N. Toropin,⁷ A. Yu. Trifonov,¹³ B. I. Vasilishin,¹³ G. Vasquez Arenas,¹⁴ P. V. Volkov,^{2,9} V. Yu. Volkov,⁹ and P. Ulloa¹⁴

(The NA64 Collaboration)

¹Universität Bonn, Helmholtz-Institut für Strahlen-und Kernphysik, 53115 Bonn, Germany

²Joint Institute for Nuclear Research, 141980 Dubna, Russia

³Technische Universität München, Physik Department, 85748 Garching, Germany

⁴CERN, European Organization for Nuclear Research, CH-1211 Geneva, Switzerland

⁵University of Illinois at Urbana Champaign, Urbana, 61801-3080 Illinois, USA

⁶UCL Department of Physics and Astronomy, University College London, Gower St., London WC1E 6BT, United Kingdom

⁷Institute for Nuclear Research, 117312 Moscow, Russia

⁸P.N. Lebedev Physical Institute, 119 991 Moscow, Russia

⁹Skobeltsyn Institute of Nuclear Physics, Lomonosov Moscow State University, 119991 Moscow, Russia

¹⁰Physics Department, University of Patras, 265 04 Patras, Greece

¹¹State Scientific Center of the Russian Federation Institute for High Energy Physics of National Research Center 'Kurchatov Institute' (IHEP), 142281 Protvino, Russia

¹²Departamento de Ciencias Físicas, Universidad Andres Bello, Sazié 2212, Piso 7, Santiago, Chile

¹³Tomsk State Pedagogical University, 634061 Tomsk, Russia

¹⁴Universidad Técnica Federico Santa María, 2390123 Valparaíso, Chile

¹⁵ETH Zürich, Institute for Particle Physics and Astrophysics, CH-8093 Zürich, Switzerland



(Received 20 January 2020; accepted 27 March 2020; published 16 April 2020)

The improved results on a direct search for a new $X(16.7 \text{ MeV})$ boson that could explain the anomalous excess of e^+e^- pairs observed in the decays of the excited ${}^8\text{Be}^*$ nuclei (“Berillium or X17 anomaly”) are reported. Interestingly, new recent results in the nuclear transitions of another nucleus, ${}^4\text{He}$, seems to support this anomaly spurring the need for an independent measurement. If the X boson exists, it could be produced in the bremsstrahlung reaction $e^-Z \rightarrow e^-ZX$ by a high energy beam of electrons incident on the active target in the NA64 experiment at the CERN Super Proton Synchrotron and observed through its subsequent decay into e^+e^- pairs. No evidence for such decays was found from the combined analysis of the data samples with total statistics corresponding to 8.4×10^{10} electrons on target collected in 2017 and 2018. This allows one to set new limits on the $X - e^-$ coupling in the range $1.2 \times 10^{-4} \lesssim e_e \lesssim 6.8 \times 10^{-4}$, excluding part of the parameter space favored by the X17 anomaly, and setting new bounds on the mixing strength of photons with dark photons (A') with a mass $\lesssim 24 \text{ MeV}$. For the 2018 run, the setup was optimized to probe the region of parameter space characterized by a large coupling e . This allowed a significant improvement in sensitivity despite a relatively modest increase in statistics.

DOI: [10.1103/PhysRevD.101.071101](https://doi.org/10.1103/PhysRevD.101.071101)

Published by the American Physical Society under the terms of the [Creative Commons Attribution 4.0 International license](https://creativecommons.org/licenses/by/4.0/). Further distribution of this work must maintain attribution to the author(s) and the published article's title, journal citation, and DOI. Funded by SCOAP³.

Dark sectors are very interesting candidates to explain the origin of dark matter (see, e.g., Ref. [1] for a recent review), whose presence has so far been inferred only through its gravitational interaction from cosmological observations [2]. If, in addition to gravity, a new force between the dark sector and visible matter exists [3,4], this

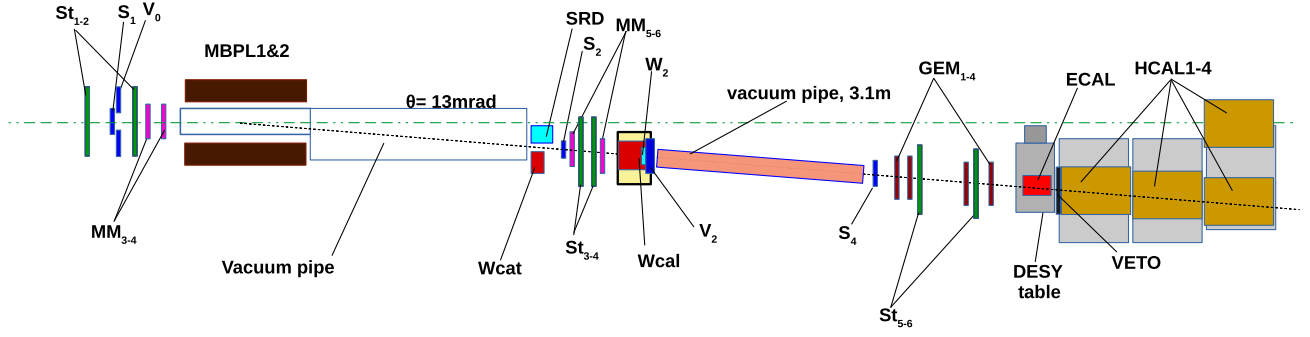


FIG. 1. The setup (2018 run) to search for $A'(X) \rightarrow e^+e^-$ decays of the bremsstrahlung $A'(X)$ produced in the reaction $eZ \rightarrow eZA'(X)$ of the 150 GeV electrons incident on the active WCAL target.

can be tested in laboratory experiments. A possibility is that this new force is carried by a vector boson A' , called dark photon. Stringent limits on the ϵ and mass $m_{A'}$ of such dark photons, excluding the parameter space region favored by the $g_\mu - 2$ anomaly have already been placed by beam dump [5–19], fixed target [20–22], collider [23–25], and rare particle decay searches [26–37].

A great boost to search for new light bosons weakly coupled to Standard Model particles was triggered by the recent observation of a $\sim 7\sigma$ excess of events in the angular distribution of e^+e^- pairs produced in the nuclear transitions of the excited ${}^8\text{Be}^*$ to its ground state via internal e^+e^- pair creation [38,39]. The latest results of the ATOMKI group report a similar excess at approximately the same invariant mass in the nuclear transitions of another nucleus, ${}^4\text{He}$ [40]. It was put forward [41,42] that this anomaly can be interpreted as the emission of a protophobic gauge boson X with a mass of 16.7 MeV decaying into e^+e^- pairs. To be consistent with the existing constraints, the X boson should have a nonuniversal coupling to quarks and a coupling strength with electrons in the range of $2 \times 10^{-4} \lesssim \epsilon_e \lesssim 1.4 \times 10^{-3}$ which translates to a lifetime of the order of $10^{-14} \lesssim \tau_X \lesssim 10^{-12}$ s.

Such a new boson could also resolve the tension between measured and predicted values of the muon anomalous magnetic moment, the so-called ($g_\mu - 2$) anomaly. The phenomenological aspects of such a light vector bosons weakly coupled to quarks and leptons were extensively studied (see, e.g., Refs. [43–56]); quite a few experimental searches were performed (see, e.g., Refs. [1,57]). Among those, the NA64 Collaboration has reported results which excluded a possible coupling strength of the X boson between $1.3 \times 10^{-4} \lesssim \epsilon_e \lesssim 4.2 \times 10^{-4}$ [58].

The NA64 experiment in the “visible mode” configuration, i.e., configured for the search for A' decaying visibly, into e^+e^- pairs, is described in [58,59] (Fig. 1). The core of the experiment consists of the two electromagnetic (EM) calorimeters: the compact target-tungsten-calorimeter (WCAL) assembled from the tungsten and plastic scintillator plates with wavelength shifting fiber readout and electromagnetic calorimeter (ECAL), a matrix of 6×6

shashlik-type lead-plastic scintillator sandwich modules [60]. The method of the search for $A' \rightarrow e^+e^-$ (or $X \rightarrow e^+e^-$) decays is detailed in Refs. [61–64]. Here we review it briefly. The $A'(X)$ is produced via scattering of high-energy electrons off nuclei of an active target-dump (WCAL in Fig. 1). Its production is followed by the decay into e^+e^- pairs,:

$$e^- + Z \rightarrow e^- + Z + A'(X), \quad A'(X) \rightarrow e^+e^-. \quad (1)$$

The active target serves as a dump to absorb the EM showers from the secondary particles emitted by the primary electrons before the $A'(X)$ production, with an energy E_s , that carry the fraction s of the primary electron energy, $s = E_s/E_0$, and the shower from the recoil electron of the reaction (1). The latter carries a fraction f of the production electron energy. The total energy that is absorbed in the WCAL is $E_{\text{WCAL}} = E_0(s + f(1 - s))$. As shown in Refs. [63,64], the value of f is peaked at zero for the most interesting masses of $A'(X)$.

The $A'(X)$ can be detected if it passes through the rest of the dump and the veto counter without interactions and decays in flight into an e^+e^- pair in the decay volume. The fraction $E_{\text{ECAL}} = E_0(1 - s)(1 - f)$ of the primary electron energy is deposited in the second downstream calorimeter ECAL, as shown in Fig. 1. In the most interesting region of the parameter space, the probability to decay after the dump significantly drops for low energy $A'(X)$ because of the short lifetime and small gamma factor; therefore, for the detectable signal events, E_{WCAL} is significantly smaller than E_0 , which means that for them $s \ll 1$. For example, at $\epsilon = 0.0006$, in 67% of the detectable signal events the deposited energy E_{WCAL} is smaller than 50 GeV (average E_{WCAL} is 38 GeV).

The occurrence of $A'(X)$ produced in the e^-Z interactions and $A' \rightarrow e^+e^-$ decays would appear as an excess of events with two EM-like showers in the setup: one shower in the WCAL and another one in the ECAL, with the total energy $E_{\text{tot}} = E_{\text{WCAL}} + E_{\text{ECAL}}$ compatible with the beam energy (E_0), above those expected from the background sources.

In order to increase the sensitivity to short-lived X bosons ($\epsilon \gtrsim 0.5 \times 10^{-4}$) as compared to the previous results several optimization steps were done in the 2018 setup (Fig. 1). Without such optimization the maximal reachable ϵ would increase only logarithmically with the number of collected electrons on target (EOT). The following changes were done: (i) The beam energy was increased to 150 GeV to boost the X boson outside the WCAL so that its decay in e^+e^- pairs can be detected; (ii) a thinner veto counter W_2 was installed immediately after the last tungsten plate inside the WCAL box to minimize the possibility for the X boson to decay before it; (iii) additional track detectors were placed between WCAL and ECAL; (iv) a vacuum pipe was installed immediately after the WCAL; (v) the distance between the WCAL and ECAL was increased; and (vi) one of the hadronic calorimeters (HCAL4) was moved on axis to act as a veto for neutral particles created upstream the magnetic spectrometer. Modifications (iii)–(v) would allow the track and vertex reconstruction of the e^+e^- pairs in case of signal observation. Modifications (iv) and (v) also serve to suppress background. As an example of the effect of these modifications, mainly (i) and (ii), the raw signal yield prediction for $\epsilon = 0.0006$ increases from 0.25 to 1.5 per 10^{10} EOT.

For the modified setup used in 2018, we have to stress the following. The purpose of the target-dump WCAL design is not to absorb the full energy E_0 of the shower generated by the primary electrons, but the energy E_{WCAL} in signal events which, as discussed above, is typically significantly smaller.

In the 2018 run, 3×10^{10} electrons on target were collected, thus including the 2017 results a total of 8.4×10^{10} events. The trigger requires in-time energy deposition in S_1 – S_3 , no energy deposition in V_0 and $E_{\text{WCAL}} \lesssim 0.7 \times E_{\text{beam}}$. The latter requirement was not applied in the runs used for calibration.

A GEANT4 [65,66]-based package was developed to perform the detailed full simulation of the experiment in order to choose the selection criteria, the calculation of the signal efficiencies, and the estimation of the background. It contains a subpackage for the simulation of various types of dark matter particles based on exact tree-level calculation of the cross sections [64].

As in the previous analyses [60,67], in order to check efficiencies and the reliability of the MC simulations, we selected a clean sample of $\simeq 10^5$ $\mu^+\mu^-$ events with $E_{\text{WCAL}} < 0.6 \times E_{\text{beam}}$ from the QED muon pair production in the dump (dimuons). This rare process is dominated by the reaction $e^-Z \rightarrow e^-Z\gamma; \gamma \rightarrow \mu^+\mu^-$ of a photon conversion into muon pair on a nucleus of the dump. We performed a number of comparisons between these events and the corresponding MC simulated sample and applied the estimated efficiency corrections to the MC events.

The candidate events are selected with the following criteria: (i) the energy deposition in the veto counter (W_2 in

2018) is $\lesssim 0.7$ *MIP* (most probable energy deposition of a minimum ionizing particle). The cut was adjusted for the different runs to take into account the variations in the energy resolution, the electronic noise, and the pileup effects in the counter; (ii) the signal in the decay counter S_4 is larger than 1.5 *MIPs*; (iii) the sum of the energies deposited in the WCAL + ECAL should be compatible with the beam energy, and at least 25 GeV should be deposited in the ECAL; (iv) the shower in the WCAL should start to develop within the first few X_0 , which is ensured by the WCAL preshower energy lower cut of 0.5 GeV; (v) the cell with maximal energy deposition in the ECAL should be the one on the beam axis after deflection in the dipole magnets; (vi) the longitudinal and lateral shapes of the shower in the ECAL are consistent with a single EM shower. The longitudinal shape is defined by requiring an energy deposition of at least 3 GeV in the ECAL pre-shower. The lateral shape of the shower was compared to the shape measured in the calibration beam using the χ^2 method. This does not decrease the efficiency for signal events because the distance between e^- and e^+ in the ECAL is significantly smaller than the ECAL cell size. (vii) Finally, the rejection of events with hadrons in the final state is based on the energy deposition in the VETO counter (less than 0.9 *MIP*) and the hadron calorimeter HCAL (less than 1 GeV for each module).

The counter W_2 is very important for this analysis. It is made using the same technology as for the tiles of the WCAL and installed inside the WCAL box to be as close as possible to the $A'(X)$ production point. The MC simulation was carefully tuned to reproduce the data. This required to take into account the following effects:

- (i) Fluctuations of the number of photoelectrons from the photocathode.
- (ii) Pulse reconstruction threshold curve for the counter below 0.8 *MIP*.
- (iii) Cross talk between the WCAL and W_2 signals. This includes contributions from the light cross talk and the electronic cross talk between the two channels. The average cross talk value was assumed to be proportional to the energy deposition in the WCAL.
- (iv) Readout electronic noise and pileup effects affecting the W_2 pulse shape.

In Fig. 2, the comparison of the MC simulation with the data for selected muons in the hadron beam and for the electron beam is shown. There is some disagreement for the electron calibration beam and for dimuons events. However, the agreement for dimuons becomes better for smaller energy deposition in the WCAL, i.e., for the conditions corresponding to signal events. The uncertainty in the definition of the W_2 threshold, conservatively taken as $\pm 30\%$, results in a systematic error in the signal efficiency estimated to be at the 10% level.

The energy deposition in W_2 expected for the detectable signal events (i.e., when the $A'(X)$ decays after the last

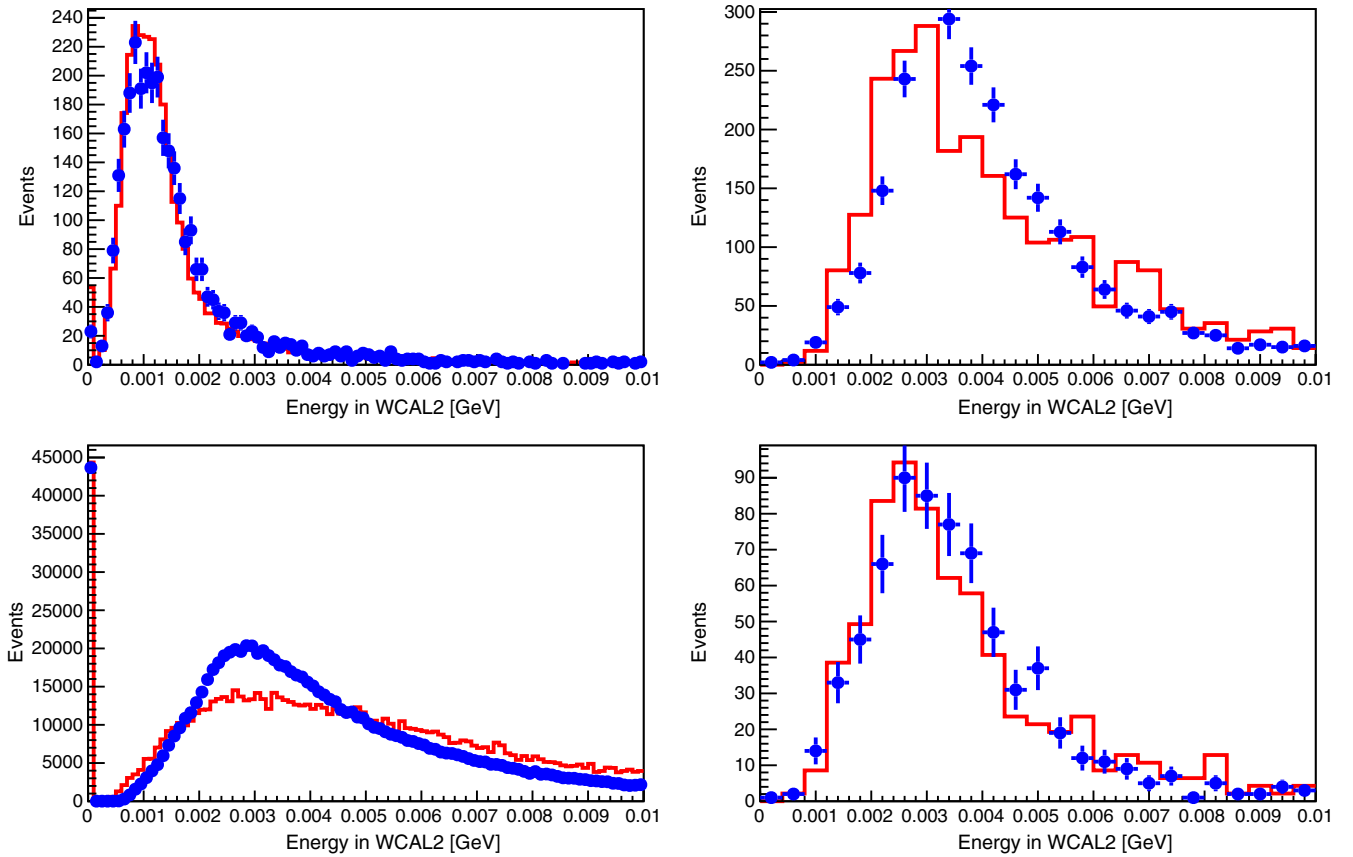


FIG. 2. The comparison of various distributions in the W_2 counter with MC predictions. Left upper plot: for muons selected in the hadron calibration beam. Right upper plot: for dimuon events with the standard cut $E_{\text{WCAL}} < 0.6 \times E_{\text{beam}}$. Right lower plot: for dimuon events with the cut $E_{\text{WCAL}} < 0.33 \times E_{\text{beam}}$. Left lower plot: for the electron calibration beam. The data and MC simulations are shown as points with error bars (blue) and histogram (red), respectively.

tungsten plate) is shown in Fig. 3. It is significantly smaller than for the electrons from the primary beam (Fig. 2, lower left plot). It is also smaller for the bigger value of ϵ since the short-lived $A'(X)$ should have higher energy for the same probability to decay after the WCAL tungsten plates, which means smaller E_{WCAL} (shorter shower).

The main background in this search comes from the $K_S^0 \rightarrow \pi^0 \pi^0$ events from K^0 mainly produced by hadrons misidentified as electrons [58]. K_0 can pass the veto counters without energy deposition and decay into $\pi^0 \pi^0$. These π^0 decay immediately into photons that can convert on some of the material of the setup (e.g., the windows of the vacuum pipe) into $e^+ e^-$ pairs and deposit energy in S_4 . The decay chain $K_S^0 \rightarrow \pi^0 \pi^0; \pi^0 \rightarrow \gamma e^+ e^-$ is also possible. We estimated this background using both simulation and data. For this, we selected the sample of “neutral” events changing the cut (ii) to $E_{S_4} < 0.5 \text{ MIP}$. The distribution of such neutral events is shown in Fig. 4. The signal box on the $E_{\text{WCAL}} - E_{\text{ECAL}}$ plot contains three events in the 2017 dataset and no events in the 2018 data. For this reason, for the estimation of background in the analysis of the 2018 data, we took a wider box changing the cut (iii) and relaxed

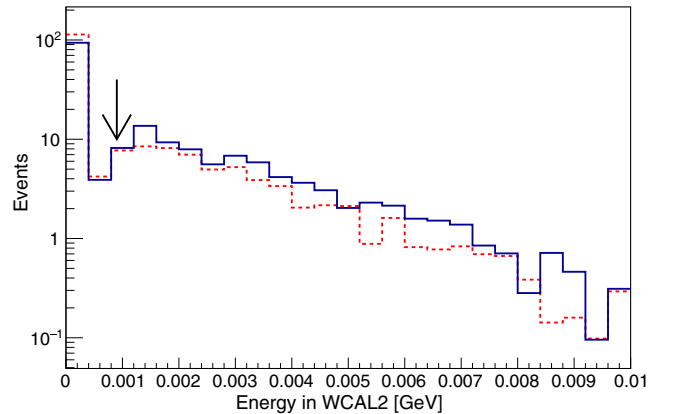


FIG. 3. The expected energy in the W_2 counter from the signal events. The upper cut value of $\lesssim 0.7 \text{ MIP}$ is shown by the arrow. Solid line histogram (blue): $\epsilon = 0.0003$, 54% of events pass the cut. Dotted line histogram (red): $\epsilon = 0.0006$, 66% of events pass the cut. The events are histogrammed with the weight corresponding to the probability for the A' to decay after the last tungsten plate of the WCAL.

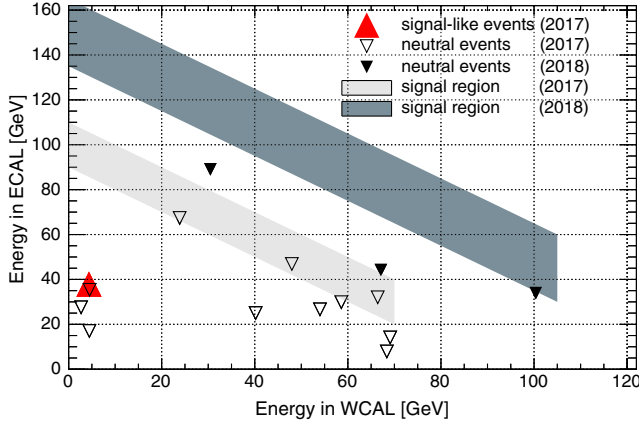


FIG. 4. Distribution of selected EM neutral and signal-like events in the $(E_{\text{WCAL}}, E_{\text{ECAL}})$ plane from 2017 to 2018 data. Neutral events are shown as hollow (2017) and full (2018) triangles. The two shadowed bands represent the signal box regions for the two different run runs. A single signal-like event detected during the 2017 run not falling into the signal region is shown with a red triangle.

the cut (vi). The MC sample of K_S^0 was simulated according to distributions predicted for the hadron interactions in WCAL. With this sample, the ratio of signal-like to neutral events is calculated resulting in the prediction of the number of background events: 0.06 for the 2017 data and 0.005 for the 2018 data (Table I). The smaller number of neutral events and lower background in the 2018 data is due to the increased distance between the WCAL and ECAL since in this configuration less K_S^0 events pass the criteria (v) and (vi). In addition, the background is decreased due to the vacuum pipe installed upstream of the S_4 .

The charge-exchange reaction $\pi^- p \rightarrow (\geq 1)\pi^0 + n + \dots$ that can occur in the last layers of the WCAL, with decay photons escaping the dump without interactions, accompanied by undetected secondaries, is another source of fake signal. To evaluate this background, we used the extrapolation of the charge-exchange cross sections, $\sigma \sim Z^{2/3}$, measured on different nuclei [68]. The beam pion flux suppression by the SRD tagging is taken into account in the estimation. Background from punchthrough π^- can

TABLE I. Expected numbers of background events in the signal box that passed the selection criteria (i)–(vi).

Source of background	2017 data	2018 data
$K_S^0 \rightarrow 2\pi^0$	0.06 ± 0.034	0.005 ± 0.003
$\pi N \rightarrow (\geq 1)\pi^0 + n + \dots$	0.01 ± 0.004	0.001 ± 0.0004
Punchthrough π^-	0.0015 ± 0.0008	0.0007 ± 0.0004
Punchthrough γ	<0.001	<0.0005
$\pi, K \rightarrow e\nu, K_{e4}$ decays		<0.001
$eZ \rightarrow eZ\mu^+\mu^-; \mu^\pm \rightarrow e^\pm\nu\bar{\nu}$		<0.001
Total	0.07 ± 0.035	0.006 ± 0.003

arise because of the inefficiency of the veto counter, mainly due to pileup. This was estimated using the simulation and the data from the calibration runs with a hadron beam. The contribution from the beam kaon decays in-flight $K^- \rightarrow e^- \nu \pi^+ \pi^- (K_{e4})$ was evaluated from simulation with a biased kaon lifetime and found to be negligible. The background from the dimuon production in the dump $e^- Z \rightarrow e^- Z \mu^+ \mu^-$ with either $\pi^+ \pi^-$ or $\mu^+ \mu^-$ pairs misidentified as EM event in the ECAL was also found to be negligible.

Table I summarizes the estimated background inside the signal box. The main part of the total background uncertainty comes from the statistical error of the number of observed EM neutral events. There is also the uncertainty from the cross sections of the π, K charge-exchange reactions on heavy nuclei (30%).

After determining and optimizing the selection criteria and estimating the background levels, we examined the signal box and found no candidates.

The combined 90% confidence level (C.L.) upper limits for the mixing strength ϵ were determined from the 90% C.L. upper limit for the expected number of signal events, $N_{A'}^{90\%}$ by using the modified frequentist approach for confidence levels, taking the profile likelihood as a test

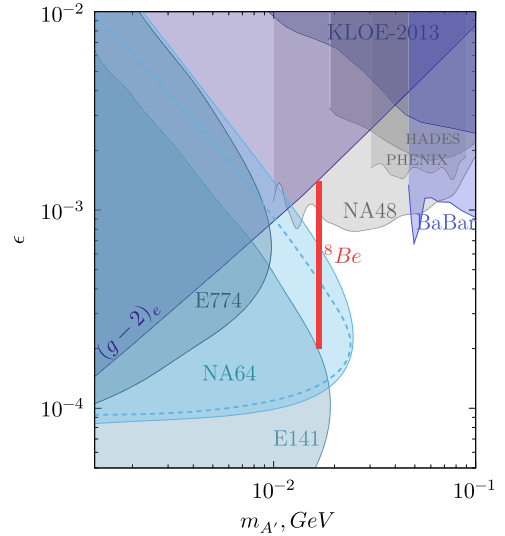


FIG. 5. The 90% C.L. exclusion areas in the $(m_X; \epsilon)$ plane from the NA64 experiment (shaded blue area) using 2017 data only (dashed line) and 2017–2018 data combined. For the mass of 16.7 MeV, the $X - e^-$ coupling region excluded by NA64 is $1.2 \times 10^{-4} < \epsilon_e < 6.8 \times 10^{-4}$. The NA48/2 limits only apply to dark photons but not the X boson because differently from the A' , it has nonuniversal couplings to u, d quarks allowing to explain the ${}^8\text{Be}^*$ anomaly [41,42]. The full allowed range of ϵ_e for the X boson, $2.0 \times 10^{-4} \lesssim \epsilon_e \lesssim 1.4 \times 10^{-3}$, is shown as a vertical red bar. The constraints on the mixing ϵ from the experiments E774 [10], E141 [7], BABAR [25], KLOE [30], HADES [32], PHENIX [33], NA48 [35], and bounds from the electron anomalous magnetic moment $(g-2)_e$ [74] are also shown.

statistic in the asymptotic approximation [69–71]. The total number of expected signal events in the signal box was the sum of expected events from the 2017 and 2018 runs,

$$N_{A'} = \sum_{i=1}^2 N_{A'}^i = \sum_{i=1}^2 n_{\text{EOT}}^i P_{\text{tot}}^i n_{A'}^i(\epsilon, m_{A'}), \quad (2)$$

where n_{EOT}^i is the effective number of EOT in run- i (5.4×10^{10} and 3×10^{10}), P_{tot}^i is the signal efficiency in the run i , and $n_{A'}^i(\epsilon, m_{A'})$ is the number of the $A' \rightarrow e^+e^-$ decays in the decay volume with energy $E_{A'} > 25$ GeV per EOT, calculated under the assumption that this decay mode is predominant; see, e.g., Eq. (3.7) in Ref. [62]. The value n_{EOT}^i takes into account the data acquisition system dead time. Each i th entry in this sum was calculated by simulating signal events for the corresponding beam running conditions and processing them through the reconstruction program with the same selection criteria and efficiency corrections as for the data sample from the run- i . In the overall signal efficiency for each run, the acceptance loss due to pileup in the veto detectors was taken into account.

The A' yield from the dump was calculated as described in Ref. [64]. These calculations were cross-checked with the calculations of Refs. [72,73]. The $\lesssim 10\%$ difference between the two calculations was accounted for as a systematic uncertainty in $n_{A'}(\epsilon, m_{A'})$. The total systematic uncertainty on $N_{A'}$ calculated by combining all uncertainties did not exceed $\simeq 25\%$ for all runs. The combined

90% C.L. exclusion limits on the mixing strength ϵ as a function of the A' mass is shown in Fig. 5 together with the constraints from other experiments. Our results set a limit on the coupling of a new X boson, which could explain the X17 anomaly, with electrons at a level of $\epsilon_e \lesssim 6.8 \times 10^{-4}$ and mass value of 16.7 MeV, leaving some unexplored region at this mass as an interesting prospect for further searches.

In accordance with the Feng model of Ref. [41], the attenuation of the X -flux due to X -neutron interactions in the WCAL target was found to be $< 1\%$, since, for the largest allowed coupling $\epsilon_n \sim 10^{-2}$ [42], the X -boson mean free path in tungsten is ~ 20 m, while the total thickness of the WCAL absorber layers is ~ 10 cm.

ACKNOWLEDGMENTS

We gratefully acknowledge the support of the CERN management and staff and the technical staffs of the participating institutions for their vital contributions. This work was supported by the Helmholtz-Institut für Strahlen- und Kernphysik, University of Bonn (Germany), JINR (Dubna), Ministry of Education and Science (Russia) and RAS (Russia), ETH Zurich and SNSF Grants No. 169133 and No. 186158 (Switzerland), FONDECYT Grants No. 1191103, No. 1190845, and No. 3170852, UTFSM PI M 18 13 and ANID PIA/APOYO AFB180002 (Chile), the Carl Zeiss Foundation 0653-2.8/581/2 (Germany), and Verbundprojekt-05A17VTA-CRESST-XENON (Germany).

-
- [1] M. Battaglieri *et al.*, [arXiv:1707.04591](https://arxiv.org/abs/1707.04591).
 - [2] G. Bertone and D. Hooper, *Rev. Mod. Phys.* **90**, 045002 (2018).
 - [3] M. Pospelov, A. Ritz, and M. B. Voloshin, *Phys. Lett. B* **662**, 53 (2008).
 - [4] M. Pospelov, *Phys. Rev. D* **80**, 095002 (2009).
 - [5] J. D. Bjorken, R. Essig, P. Schuster, and N. Toro, *Phys. Rev. D* **80**, 075018 (2009).
 - [6] F. Bergsma *et al.* (CHARM Collaboration), *Phys. Lett. B* **166**, 473 (1986).
 - [7] E. M. Riordan *et al.* *Phys. Rev. Lett.* **59**, 755 (1987).
 - [8] J. D. Bjorken, S. Ecklund, W. R. Nelson, A. Abashian, C. Church, B. Lu, L. W. Mo, T. A. Nunamaker, and P. Rassmann, *Phys. Rev. D* **38**, 3375 (1988).
 - [9] A. Konaka *et al.*, *Phys. Rev. Lett.* **57**, 659 (1986).
 - [10] A. Bross, M. Crisler, S. H. Pordes, J. Volk, S. Errede, and J. Wrbanek, *Phys. Rev. Lett.* **67**, 2942 (1991).
 - [11] M. Davier and H. N. Ngoc, *Phys. Lett. B* **229**, 150 (1989).
 - [12] C. Athanassopoulos *et al.* (LSND Collaboration), *Phys. Rev. C* **58**, 2489 (1998).
 - [13] P. Astier *et al.* (NOMAD Collaboration), *Phys. Lett. B* **506**, 27 (2001).
 - [14] S. Adler *et al.* (E787 Collaboration), *Phys. Rev. D* **70**, 037102 (2004).
 - [15] R. Essig, R. Harnik, J. Kaplan, and N. Toro, *Phys. Rev. D* **82**, 113008 (2010).
 - [16] J. Blumlein and J. Brunner, *Phys. Lett. B* **701**, 155 (2011).
 - [17] S. N. Gninenko, *Phys. Lett. B* **713**, 244 (2012).
 - [18] J. Blumlein and J. Brunner, *Phys. Lett. B* **731**, 320 (2014).
 - [19] S. Andreas, C. Niebuhr, and A. Ringwald, *Phys. Rev. D* **86**, 095019 (2012).
 - [20] S. Abrahamyan *et al.* (APEX Collaboration), *Phys. Rev. Lett.* **107**, 191804 (2011).
 - [21] H. Merkel *et al.*, *Phys. Rev. Lett.* **112**, 221802 (2014).
 - [22] H. Merkel *et al.* (A1 Collaboration), *Phys. Rev. Lett.* **106**, 251802 (2011).
 - [23] B. Aubert *et al.* (BABAR Collaboration), *Phys. Rev. Lett.* **103**, 081803 (2009).
 - [24] D. Curtin *et al.*, *Phys. Rev. D* **90**, 075004 (2014).
 - [25] J. P. Lees *et al.* (BABAR Collaboration), *Phys. Rev. Lett.* **113**, 201801 (2014).

- [26] G. Bernardi, G. Carugno, J. Chauveau, F. Dicarolo, M. Dris *et al.*, *Phys. Lett. B* **166**, 479 (1986).
- [27] R. M. Drees *et al.* (SINDRUM I Collaboration), *Phys. Rev. Lett.* **68**, 3845 (1992).
- [28] F. Archilli *et al.* (KLOE-2 Collaboration), *Phys. Lett. B* **706**, 251 (2012).
- [29] S. N. Gninenko, *Phys. Rev. D* **85**, 055027 (2012).
- [30] D. Babusci *et al.* (KLOE-2 Collaboration), *Phys. Lett. B* **720**, 111 (2013).
- [31] P. Adlarson *et al.* (WASA-at-COSY Collaboration), *Phys. Lett. B* **726**, 187 (2013).
- [32] G. Agakishiev *et al.* (HADES Collaboration), *Phys. Lett. B* **731**, 265 (2014).
- [33] A. Adare *et al.* (PHENIX Collaboration), *Phys. Rev. C* **91**, 031901 (2015).
- [34] A. V. Artamonov *et al.* (BNL-E949 Collaboration), *Phys. Rev. D* **79**, 092004 (2009).
- [35] J. R. Batley *et al.* (NA48/2 Collaboration), *Phys. Lett. B* **746**, 178 (2015).
- [36] V. V. Dubinina, N. P. Egorenkova, E. A. Pozharova, N. G. Polukhina, V. A. Smirniysky, and N. I. Starkov, *Yad. Fiz.* **80**, 245 (2017) [*Phys. At. Nucl.* **80**, 461 (2017)].
- [37] A. Anastasi *et al.* (KLOE-2 Collaboration), *Phys. Lett. B* **757**, 356 (2016).
- [38] A. Krasznahorkay *et al.*, *Phys. Rev. Lett.* **116**, 042501 (2016).
- [39] A. J. Krasznahorkay *et al.*, *J. Phys. Conf. Ser.* **1056**, 012028 (2018).
- [40] A. J. Krasznahorkay *et al.*, arXiv:1910.10459v1; N. V. Krasnikov, arXiv:1912.11689.
- [41] J. L. Feng, B. Fornal, I. Galon, S. Gardner, J. Smolinsky, T. M. P. Tait, and P. Tanedo, *Phys. Rev. Lett.* **117**, 071803 (2016).
- [42] J. L. Feng, B. Fornal, I. Galon, S. Gardner, J. Smolinsky, T. M. P. Tait, and P. Tanedo, *Phys. Rev. D* **95**, 035017 (2017).
- [43] J. Kozaczuk, *Phys. Rev. D* **97**, 015014 (2018).
- [44] C.-W. Chiang and P.-Y. Tseng, *Phys. Lett. B* **767**, 289 (2017).
- [45] X. Zhang and G. A. Miller, *Phys. Lett. B* **773**, 159 (2017).
- [46] I. Alikhanov and E. A. Paschos, *Phys. Rev. D* **97**, 115004 (2018).
- [47] Y. Liang, L.-B. Chen, and C.-F. Qiao, *Chin. Phys. C* **41**, 063105 (2017).
- [48] B. Fornal, *Int. J. Mod. Phys. A* **32**, 1730020 (2017).
- [49] L. B. Okun, *Zh. Eksp. Teor. Fiz.* **83**, 892 (1982) [*Sov. Phys. JETP* **56**, 502 (1982)], <http://www.jetp.ac.ru/cgi-bin/elindex/e/56/3/p502?a=list>.
- [50] P. Galison and A. Manohar, *Phys. Lett. B* **136**, 279 (1984).
- [51] B. Holdom, *Phys. Lett. B* **166**, 196 (1986).
- [52] P. Fayet, *Eur. Phys. J. C* **77**, 53 (2017).
- [53] P. Fayet, *Nucl. Phys.* **B187**, 184 (1981).
- [54] P. Fayet, *Nucl. Phys.* **B347**, 743 (1990).
- [55] P. Fayet, *Phys. Rev. D* **75**, 115017 (2007).
- [56] J. Jaeckel and A. Ringwald, *Annu. Rev. Nucl. Part. Sci.* **60**, 405 (2010).
- [57] E. Nardi, C. D. R. Carvajal, A. Ghoshal, D. Meloni, and M. Raggi, *Phys. Rev. D* **97**, 095004 (2018).
- [58] D. Banerjee *et al.* (NA64 Collaboration), *Phys. Rev. Lett.* **120**, 231802 (2018).
- [59] D. Banerjee *et al.*, *Nucl. Instrum. Methods Phys. Res., Sect. A* **881**, 72 (2018).
- [60] D. Banerjee *et al.* (NA64 Collaboration), *Phys. Rev. D* **97**, 072002 (2018).
- [61] S. N. Gninenko, *Phys. Rev. D* **89**, 075008 (2014).
- [62] S. Andreas *et al.*, *Phys. Rev. D* **89**, 075008 (2014).
- [63] S. N. Gninenko, N. V. Krasnikov, M. M. Kirsanov, and D. V. Kirpichnikov, *Phys. Rev. D* **94**, 095025 (2016).
- [64] S. N. Gninenko, D. V. Kirpichnikov, M. M. Kirsanov, and N. V. Krasnikov, *Phys. Lett. B* **782**, 406 (2018).
- [65] S. Agostinelli *et al.* (GEANT4 Collaboration), *Nucl. Instrum. Methods Phys. Res., Sect. A* **506**, 250 (2003).
- [66] J. Allison *et al.*, *IEEE Trans. Nucl. Sci.* **53**, 270 (2006).
- [67] D. Banerjee *et al.* (NA64 Collaboration), *Phys. Rev. Lett.* **118**, 011802 (2017).
- [68] V. N. Bolotov, V. V. Isakov, V. A. Kachanov, D. B. Kakauridze, V. M. Kutyin, Y. D. Prokoshkin, E. A. Razuvaev, and V. K. Semenov, *Nucl. Phys.* **B85**, 158 (1975).
- [69] T. Junk, *Nucl. Instrum. Methods Phys. Res., Sect. A* **434**, 435 (1999).
- [70] G. Cowan, K. Cranmer, E. Gross, and O. Vitells, *Eur. Phys. J. C* **71**, 1554 (2011).
- [71] A. L. Read, *J. Phys. G* **28**, 2693 (2002).
- [72] Y. S. Liu, D. McKeen, and G. A. Miller, *Phys. Rev. D* **95**, 036010 (2017).
- [73] Y. S. Liu and G. A. Miller, *Phys. Rev. D* **96**, 016004 (2017).
- [74] H. Davoudiasl, H. S. Lee, and W. J. Marciano, *Phys. Rev. D* **89**, 095006 (2014).